CrossMark

Nano-sized Cu/Zn-modified MCM-41 (Cu/Zn-MCM-41): preparation, characterization and catalytic application in a new more atom efficient synthesis of tetrasubstituted imidazoles

Mohsen Shekouhy[1] · Ali Moaddeli[1] · Ali Khalafi-Nezhad[1]

Abstract The nano-sized copper/zinc-modified MCM-41 (Cu/Zn-MCM-41) was successfully prepared, characterized and applied as a new heterogeneous mesoporous and reusable nano-catalyst in a more atom efficient and novel one-pot three component strategy for the synthesis of tetrasubstituted imidazoles from nitriles, amines and benzoins under microwave irradiation. Using this method, the major problem of previously reported method (application of toxic and non-recoverable trifluoroacetic acid (TFA) as a catalyst) have been solved and all obtained results were highly similar (reaction times and yields) to the application of TFA that proved the efficiency of prepared catalyst in titled reaction.

Keywords Tetrasubstituted imidazoles · Nano-sized copper/zinc-modified MCM-41 · Mesoporous catalyst · Multi-component reaction · One-pot synthesis

1 Introduction

Nowadays the application of heterogeneous catalysis instead of liquid acid catalysts and no recoverable traditional inorganic bases has become a useful strategy in the development of more benign and environmental friendly processes in organic synthesis [1]. Between various kinds of heterogeneous catalytic systems, mesoporous materials have attracted much attentions due to their unique characteristics such as high thermal, chemical and mechanical stability, high surface area, tunable pore sizes and uniform porosity and free diffusion of reactants and products to the active catalytic sites [2]. Between various types of mesoporous compounds, MCM-41 as a periodic mesoporous silica material has attracted much attention and has been studied for the synthesis of various heterogeneous catalysts and has been frequently applied as a support in organic processes [3–6]. It is noteworthy that the application of MCM-41 provides ideal conditions for organic reactions because it has high surface area and uniform two dimensional hexagonal channels and selectively controllable pore sizes in the range of 2–10 nm, however, its catalytic activity is low due to the lack of potent acid or base active sites [7–9]. There are various reported strategies for the modification of MCM-41 with the aim of enhancement of its catalytic activity [10–14]. One of the most useful and frequently used methods to gain modified MCM-41 with enhanced catalytic activity is the replacement of some Si atoms with transition metals [15–21].

Imidazoles as an important class of heterocyclic compounds can be found in chemical structure of some important biological active compounds such as histidine, histamine, biotin and important natural products such as pilocarpine alkaloids [22]. Besides, there are numerous synthesized imidazoles with unique bioactivities such as anti-allergenic [23], anti-inflammatory [24], antifungal, antimycotic, antibiotic, antiulcerative, antibacterial and antitumoral [25]. Between various imidazole derivatives, highly substituted imidazoles have attracted more attention and their preparation and biological activities have been studied by many research groups [26–46]. More recently we introduce a novel and more atom efficient method for the synthesis of tetrasubstituted imidazoles via a one-pot three-component condensation of benzoin, nitriles and amines in the presence of trifluoroacetic acid (TFA) under microwave

✉ Ali Khalafi-Nezhad
khalafi@chem.susc.ac.ir

[1] Department of Chemistry, College of Sciences, Shiraz University, Shiraz 71454, Iran
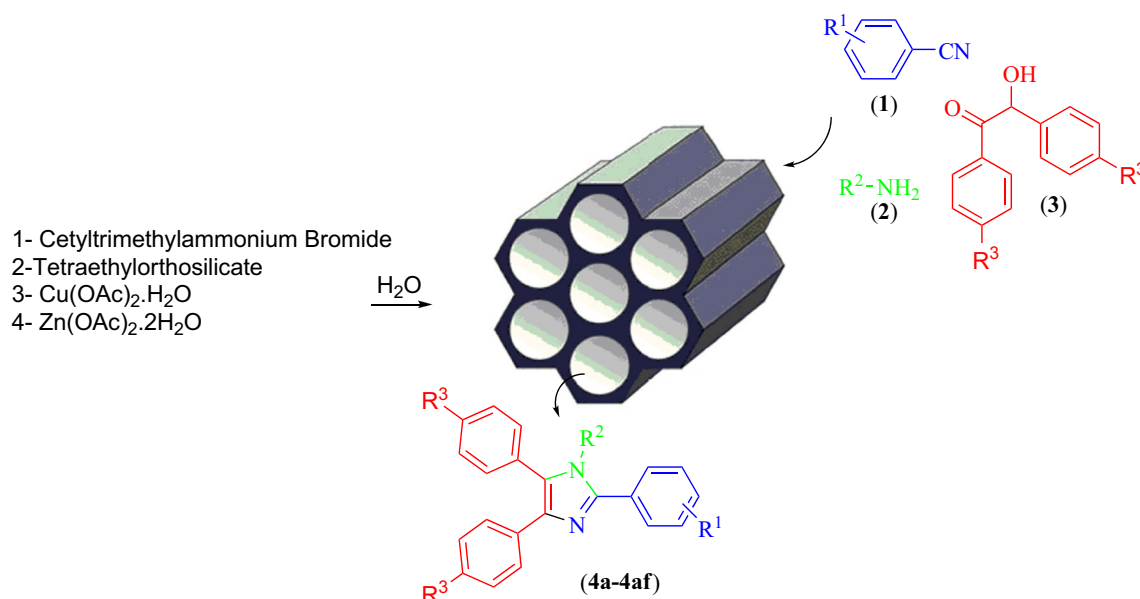
irradiation [47]. This is noteworthy that the application of this method is in combination with some highlighted advantages such as higher atom efficiencies, application of highly efficient energy source, very short reaction times (6–18 min) and high yields (83–91%) of products, but, it is in combination with a crucial drawback, the application of TFA that is a highly toxic [$LD_{50} = 200$ mg/kg (oral rat)] and no recoverable material that will cause to the production of harmful waste. So, there still exists a demand for devising more environmentally benign, recoverable and reusable catalytic systems for the one-pot condensation of benzoin, nitriles and amine as a more atom efficient approach to tetrasubstituted imidazoles.

Based on the above facts and as a part of our recent studies in the development of more benign catalytic systems in organic synthesis [48–53], we herein report the preparation of nano-sized Cu/Zn-modified MCM-41 as a new highly efficient and reusable mesoporous nano-catalyst for the synthesis of tetrasubstituted imidazoles via a one-pot condensation of nitriles (1), amines (2) and benzoins (3) (Scheme 1).

2 Experimental

All chemicals were purchased from international chemical companies (Merck, Sigma-Aldrich and Fluka) and were applied directly without further purifications. ^{1}H and ^{13}C NMR spectra were recorded on a Bruker Avance (250 MHz for ^{1}H and 62.5 MHz for ^{13}C) spectrometer with tetramethylsilane (TMS) as an internal standard and in DMSO-d_6 as solvent. A Bruker FT-IR Equinax-55 spectrophotometer was applied in order to report the infrared spectra. All XRD patterns were recorded on a Bruker D8 ADVANCE X-ray diffractometer with the nickel filtered Cu Kα radiation (λ = 1.5406 Å). The KYKY-EM3200 instrument was applied for the preparation of scanning electron micrograms (SEM). Transmittance electron microscopy (TEM) was performed with Zeiss-EM10C at 80 KV. A laboratory microwave oven (MicroSYNTH, Milestone Company, Italy) was applied as microwave irradiator. The reactions were performed in a high pressure resistance glass tube sealed with a septum. A calibrated infrared temperature control sensor mounted under the reaction vessel was applied to monitor the reaction temperature and the reaction mixture was magnetically stirred during the microwave irradiation. Melting points were determined in open capillary tubes with a Büchi B-545 melting point apparatus. Microanalysis was performed on a Perkin-Elmer 240-B microanalyzer (the classical Pregl–Dumas method where samples are combusted in a pure oxygen environment, with the resultant combustion gases measured in an automated fashion has been applied. samples encapsulated in tin or aluminum vials are inserted automatically from the integral 60-position autosampler (solid compounds). For CHN analysis, the combusted sample then goes through a reduction chamber to a homogenization chamber. The resultant gases are separated using frontal chromatography, then elute through a thermal conductivity detector using He as a neutral eluent).

1- Cetyltrimethylammonium Bromide
2- Tetraethylorthosilicate
3- Cu(OAc)$_2$.H$_2$O
4- Zn(OAc)$_2$.2H$_2$O

Scheme 1 The preparation of nano-sized Cu/Zn-modified MCM-41 for the synthesis of tetrasubstituted imidazoles (4) via a one-pot condensation of nitriles (1), amines (2) and benzoins (3)

2.1 The preparation of nano-sized Cu/Zn-MCM-41

The method of direct insertion of Cu and Zn ions in the sol gel preparation step was applied for the synthesis of nano-sized Cu/Zn-MCM-41. For this, a gel composition (molar ratio) of SiO_2:CTAB:NH_4OH:H_2O:Cu$(OAc)_2·H_2O$:Zn$(OAc)_2·2H_2O = 1.000:0.127:0.623:508.000:0.033:0.033$ [tetraethyl orthosilicate (TEOS) as the Si source, cetyltrimethylammonium bromide (CTAB) as the template, ammonia as the pH control agent, Cu$(OAc)_2·H_2O$ as the copper source and Zn$(OAc)_2·2H_2O$ as the zinc source] was applied for typical synthesis of Cu/Zn-MCM-41 with both Si/Cu and Si/Zn molar ratios of 30 and $1.000:0.127:0.623:508.000:0.033:0.0165$ for typical synthesis of Cu/Zn-MCM-41 with Si/Cu and Si/Zn molar ratios of 30 and 60 respectively.

In a typical procedure for the synthesis of Cu/Zn-MCM-41 with both Si/Cu and Si/Zn molar ratios of 30, the solution of cetyltrimethylammonium bromide (1040 mg) in deionized water (200 mL) was vigorously stirred at 60 °C for 15 min. Tetraethyl orthosilicate (5 mL) was added dropwise during 60 min gradually followed by dropwise addition of the solution of Cu$(OAc)_2·H_2O$ (150 mg) and Zn$(OAc)_2·2H_2O$ (165 mg) in 5 mL of deionized water. The obtained mixture was vigorous stirred for 1 h at 25 °C. After this time, the pH of the solution was adjusted to 10.5 with the addition of 25 wt% ammonia and obtained mixture was stirred for 12 h at 25 °C. The gel was separated by centrifugation, washed with ethanol (20 mL) and deionized water (40 mL), dried at 120 °C for 2 h and calcined in air at 550 °C for 4 h. This procedure was also applied for the preparation of Cu/Zn-MCM-41 with Si/Cu molar ratio of 30 and Si/Zn molar ratio of 60 and only 82 mg of Zn$(OAc)_2·2H_2O$ was applied. Similarly, Cu/Zn-MCM-41 with Si/Cu molar ratio of 60 and Si/Zn molar ratio of 30 was prepared with the application of Cu$(OAc)_2·H_2O$ (75 mg) and Zn$(OAc)_2·2H_2O$ (165 mg). The Cu-MCM-41-30 and Zn-MCM-41-30 were prepared based on a reported procedure [54]. The obtained samples were named as Cu/Zn-MCM-41-x-y where x and y are the Si/Cu and Si/Zn molar ratios in their initial gel compositions, respectively. Please note: the selection of metal concentration in MCM-41 framework depends on two important factors: (1) maximum amount of metal to reach high active sites and (2) high crystallinity and high surface area of final composite. Substitution of the structural Si^{4+} by the Cu^{2+} and Zn^{2+} ions, resulting in partial collapse of the hexagonal structure of MCM-41 and the increase in unit-cell parameters. These results are probably due to the larger size of ions compared to the Si^{4+}. This earlier case was investigated in our previous work about copper modified MCM-41. So that optimized ion concentration in this work has been selected base on the previous

results, textural and catalytic behaviour of the prepared catalysts with various Si/ion molar ratios [54].

2.2 General procedure for the synthesis of tetrasubstituted imidazoles

In a pressure-resistance microwave glass tube, nitriles (**1**) (1 mmol), amines (**2**) (1 mmol), benzoins (**3**) (1 mmol) and Cu/Zn-MCM-41 (20 mg) were added and sealed carefully with a septum. In order to mix the reactants and catalyst, the mixture was stirred for 5 min at room temperature and then exposed to microwave irradiation (300 W) at 90 °C (The microwave instrument automatically increased the temperature to 90 °C during 1 min) and the completion of the reaction was followed by TLC. After the completion of reaction, the mixture was cooled to room temperature, ethyl acetate (20 mL) was added and resulting mixture was stirred magnetically at 80 °C for 5 min. Insoluble catalyst was separated with centrifugation, washed with ethyl acetate (10 mL, two times), dried at 120 °C for 2 h, calcined at 550 °C for 2 h and reused. The catalyst almost completely (>99%) has been recovered from the reaction media. The separated solution was kept at room temperature for 48 h and precipitated crystals were filtered and dried under reduced pressure to afford pure products.

2.2.1 1-(4-Isopropylphenyl)-2,4,5-triphenyl-1H-imidazole (4b)

White powder, ^1H NMR (250 MHz, DMSO-d_6) δ (ppm) 1.08 (d, $J = 7.0$ Hz, 6H), 2.84 (Septet, $J = 5.5$ Hz, 1H), 7.15–7.48 (m, 19H). ^{13}C NMR (62.5 MHz, DMSO-d_6) δ (ppm) 22.8, 32.5, 123.3, 124.1, 126.5, 127.1, 127.6, 128.0, 128.8, 128.5, 129.0, 129.4, 129.5, 130.0, 130.3, 130.8, 132.6, 133.2, 135.9, 144.6, 146.4. Anal. Calcd. for $C_{30}H_{26}N_2$: C, 86.92; H, 6.32; N, 6.76 (%). Found: C, 86.88; H, 6.30; N, 6.79 (%).

2.2.2 1-Benzyl-2,4,5-triphenyl-1H-imidazole (4d)

White powder, ^1H NMR (250 MHz, DMSO-d_6) δ (ppm) 5.14 (s, 2H), 6.71–7.66 (m, 20H). ^{13}C NMR (62.5 MHz, DMSO-d_6) δ (ppm) 50.2, 126.7, 127.2, 127.4, 127.8, 128.3, 128.5, 128.8, 128.9, 129.2, 129.6, 129.7, 129.9, 130.0, 131.2, 132.4, 132.9, 136.7, 142.3, 150.9. Anal. Calcd. for $C_{28}H_{22}N_2$: C, 87.01; H, 5.74; N, 7.25 (%). Found: C, 86.95; H, 5.71; N, 7.33 (%).

2.2.3 1-(4-Methoxyphenyl)-2,4,5-triphenyl-1H-imidazole (4e)

White powder, ^1H NMR (250 MHz, DMSO-d_6) δ (ppm) 3.67 (s, 3H), 6.80–7.36 (m, 19H). ^{13}C NMR (62.5 MHz,

DMSO-d_6) δ (ppm) 53.4, 114.3, 123.4, 127.3, 128.1, 128.4, 128.6, 128.8, 129.1, 129.4, 129.7, 130.1, 130.4, 130.7, 131.0, 133.0, 133.52, 133.59, 146.2, 158.4. Anal. Calcd. for $C_{28}H_{22}N_2O$: C, 83.56; H, 5.51; N, 6.96 (%). Found: C, 83.48; H, 5.45; N, 7.01 (%).

2.2.4 4-(1-Benzyl-4,5-diphenyl-1H-imidazol-2-yl)phenol (4p)

White powder, ^{1}H NMR (250 MHz, DMSO-d_6) δ (ppm) 5.06 (s, 2H), 6.70–7.44 (m, 19H), 9.80 (s, 1H). ^{13}C NMR (62.5 MHz, DMSO-d_6) δ (ppm) 49.7, 116.3, 123.7, 126.9, 127.5, 127.7, 128.3, 128.66, 128.69, 128.8, 129.11, 129.18, 129.3, 129.6, 132.0, 134.5, 136.7, 141.5, 150.8, 158.7. Anal. Calcd. for $C_{28}H_{22}N_2O$: C, 83.56; H, 5.51; N, 6.96 (%). Found: C, 83.60; H, 5.62; N, 7.05 (%).

2.2.5 4-(1,4,5-Triphenyl-1H-imidazol-2-yl)phenol (4q)

White powder, ^{1}H NMR (250 MHz, DMSO-d_6) δ (ppm) 6.61–6.66 (m, 2H), 7.10–7.43 (m, 17H), 9.70 (s, 1H). ^{13}C NMR (62.5 MHz, DMSO-d_6) δ (ppm) 116.0, 123.7, 125.9, 127.0, 127.6, 128.0, 128.5, 128.8, 129.0, 129.3, 129.5, 129.8, 130.7, 133.2, 133.4, 136.2, 141.6, 158.8. Anal. Calcd. for $C_{27}H_{20}N_2O$: C, 83.48; H, 5.19; N, 7.21 (%). Found: C, 83.44; H, 5.21; N, 7.25 (%).

2.2.6 4-(1-(4-Methoxyphenyl)-4,5-diphenyl-1H-imidazol-2-yl)phenol (4r)

White powder, ^{1}H NMR (250 MHz, DMSO-d_6) δ (ppm) 3.77 (s, 3H), 6.73 (d, $J = 8.5$ Hz, 2H), 6.96 (d, $J = 8.5$ Hz, 2H), 7.23–7.64 (m, 14H), 9.62 (br, 1H). ^{13}C NMR (62.5 MHz, DMSO-d_6) δ (ppm) 54.5, 114.5, 115.7, 124.8, 126.2, 126.7, 128.0, 128.5, 129.2, 129.4, 129.5, 129.7, 131.0, 132.8, 133.10, 133.19, 149.2, 158.3, 159.0. Anal. Calcd. for $C_{28}H_{22}N_2O_2$: C, 80.36; H, 5.30; N, 6.69 (%). Found: C, 80.41; H, 5.36; N, 6.63 (%).

2.2.7 4-(1-(4-Chlorophenyl)-4,5-diphenyl-1H-imidazol-2-yl)phenol (4s)

White powder, ^{1}H NMR (250 MHz, DMSO-d_6) δ (ppm) 6.67–6.72 (m, 2H), 7.15–7.40 (m, 16H), 9.66 (br, 1H). ^{13}C NMR (62.5 MHz, DMSO-d_6) δ (ppm) 116.2, 123.5, 125.5, 126.8, 128.8, 128.9, 129.0, 129.2, 129.4, 129.6, 129.7, 130.1, 130.4, 133.0, 133.2, 133.9, 136.4, 147.0, 159.0. Anal. Calcd. for $C_{27}H_{19}ClN_2O$: C, 76.68; H, 4.53; N, 6.62 (%). Found: C, 76.60; H, 4.59; N, 6.70 (%).

2.2.8 1-Benzyl-2-(4-methoxyphenyl)-4,5-diphenyl-1H-imidazole (4t)

White powder, ^{1}H NMR (250 MHz, DMSO-d_6) δ (ppm) 2.26 (s, 3H), 5.10 (s, 2H), 6.63–7.50 (m, 19H). ^{13}C NMR (62.5 MHz, DMSO-d_6) δ (ppm) 47.6, 53.0, 112.1, 123.5, 127.0, 127.4, 127.6, 128.56, 128.58, 128.7, 129.0, 129.2, 129.5, 129.7, 131.0, 132.2, 132.9, 137.4, 140.7, 152.3, 160.8. Anal. Calcd. for $C_{29}H_{24}N_2O$: C, 83.63; H, 5.81; N, 6.73 (%). Found: C, 83.70; H, 5.89; N, 6.70 (%).

2.2.9 2-(4-Tert-butylphenyl)-1-benzyl-4,5-diphenyl-1H-imidazole (4u)

White powder, ^{1}H NMR (250 MHz, DMSO-d_6) δ (ppm) 1.26 (s, 9H), 5.10 (s, 2H), 6.70–7.49 (m, 19H). ^{13}C NMR (62.5 MHz, DMSO-d_6) δ (ppm) 29.6, 33.5, 28.0, 124.0, 125.9, 126.4, 126.6, 127.3, 127.5, 127.6, 127.8, 128.0, 128.3, 128.5, 128.7, 131.4, 131.7, 135.1, 140.7, 150.0, 150.4. Anal. Calcd. for $C_{32}H_{30}N_2$: C, 86.84; H, 6.83; N, 6.33 (%). Found: C, 86.76; H, 6.91; N, 6.30 (%).

2.2.10 2-(4-(1-Benzyl-4,5-diphenyl-1H-imidazol-2-yl)phenyl)-1H-benzo[d]imidazole (4x)

White powder, ^{1}H NMR (250 MHz, DMSO-d_6) δ (ppm) 6.50 (s, 2H), 6.83–7.69 (m, 23H), 12.90 (s, 1H). ^{13}C NMR (62.5 MHz, DMSO-d_6) δ (ppm) 46.6, 113.0, 115.0, 120.3, 120.5, 124.0, 125.1, 125.2, 125.3, 125.9, 126.0, 126.2, 126.3, 126.5, 126.6, 127.0, 127.1, 127.2, 127.6, 130.4, 130.9, 134.0, 138.7, 139.4, 149.0, 153.5. Anal. Calcd. for $C_{35}H_{26}N_4$: C, 83.64; H, 5.21; N, 11.15 (%). Found: C, 83.57; H, 5.17; N, 11.18 (%).

3 Results and discussion

In the first step, nano-sized copper/zinc-modified MCM-41 was prepared as a new mesoporous heterogeneous catalyst with the direct insertion of the Cu and Zn ions in the sol–gel preparation step at ambient temperature and the structure of synthesized catalyst was fully characterized with XRD, IR, SEM, TEM, ICP and BET methods. In this case, two samples of Cu/Zn-MCM-41 with different Si/Cu and Si/Zn molar ratios were prepared and their structures were compared with the structures of MCM-41 and Cu-MCM-41.

In low angle XRD patterns, the main peaks, related to the [100] reflection of MCM-41, Cu-MCM-41-30, Cu/Zn-MCM-41-30-60 and Cu/Zn-MCM-41-30-30 are observed in 2θ = 2.4°, 1.45°, 2.32° and 2.2°, respectively (Fig. 1). Presence of the Cu atoms in the MCM-41 framework causes the increasing d-spacing factor and due to
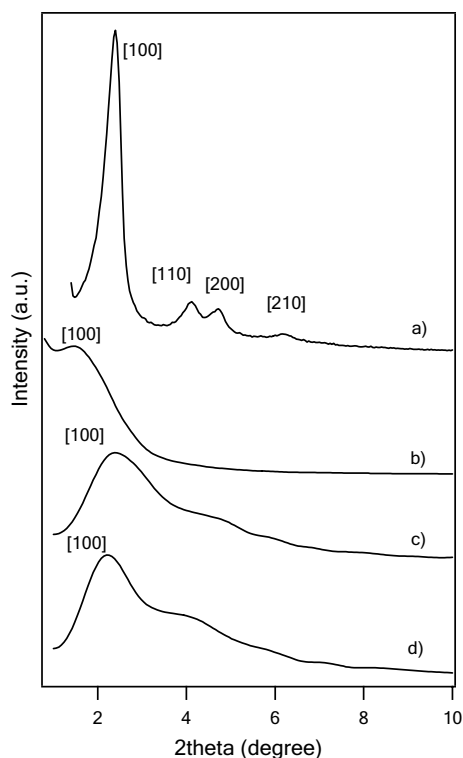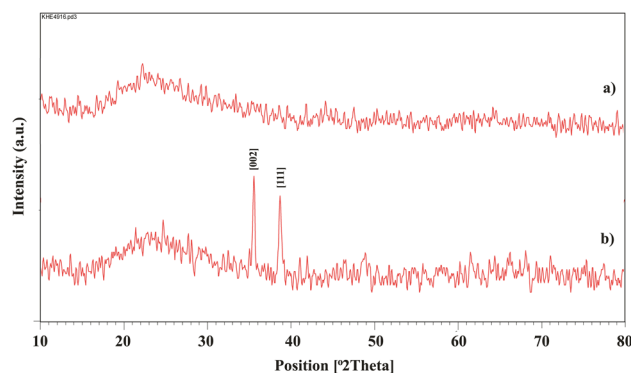
Fig. 1 Low angle XRD patterns of *(a)* MCM-41, *(b)* Cu-MCM-41-30, *(c)* Cu/Zn-MCM-41-30-60 and *(d)* Cu/Zn-MCM-41-30-30

an expansion in MCM-41 mesopores, Cu/Zn-MCM-41 samples show nearer *d*-spacing factors than Cu-MCM-41 with equal Si/Cu molar ratio base on the [100] reflection angle respect to the pure MCM-41. Nevertheless, Cu/Zn-MCM-41 sample with higher Cu/Zn molar ratio shows a larger *d*-spacing factor. In addition, the intensities of the main peaks of ion incorporated MCM-41 samples were decreased gradually with increasing of metal ion content in the samples. The incorporation of the Cu and Zn into the hexagonal channels of MCM-41 was lead to the decrease in the long-range order of the hexagonal meso-structure of MCM-41. It can be concluded from these observation that the presence of these ions partially destroys the crystalline structure of MCM-41.

As it is shown in Fig. 2, high angle XRD pattern of Cu/Zn-MCM-41-30-30 shows slight extent of CuO with tenorite phase. Surprisingly, with decreasing the Zn content, tenorite phase is vanished in Cu/Zn-MCM-41-30-60. And also, a distinct phase for ZnO is not found in the XRD pattern of Cu/Zn-MCM-41 samples. Overall, these facts show high dispersion of copper and zinc ions in the MCM-41 framework.

The mesopore structure of prepared Cu/Zn-MCM-41-30-30 was studied by TEM and compared with the TEM of MCM-41 and Zn-MCM-41-30. The

Fig. 2 The high angle XRD patterns of *(a)* Cu/Zn-MCM-41-30-60 and *(b)* Cu/Zn-MCM-41-30-30

TEM images of the Cu/Zn-MCM-41-30-30 (Fig. 3c), Zn-MCM-41-30 (Fig. 3b) and Cu-MCM-41-30 (For TEM image please see [54]) show very well the porosity of prepared materials in the range of mesoporous compounds (Fig. 3). There is partially non-uniform pore size distribution in Cu/Zn-MCM-41-30-30, Zn-MCM-41-30 and Cu-MCM-41-30 and this comes from the incorporation of the Cu and/or Zn atoms in the MCM-41 framework that is in good agreement with XRD data.

The FT-IR spectra of pure MCM-41 and Cu and Zn-incorporated MCM-41 samples are shown in Fig. 4. In IR spectrum of MCM-41 there are three characteristic peaks at 460, 808, and 1089 cm^{-1} corresponding to the rocking, bending (or symmetric stretching), and asymmetric stretching of the inter-tetrahedral oxygen atoms in SiO_2, respectively. The peak at 966 cm^{-1} is assigned to the silanol group (Si–OH) (Fig. 4a).

A slight red shift, related to the vibration absorption band at 1089 cm^{-1} corresponding to v (Si–O–Si), to the lower frequencies in the spectra of ion incorporated MCM-41 samples indicates the formation of Si–O-ion bond and incorporation of the Cu and Zn in the framework of MCM-41 (Fig. 4b, c).

The particle size and morphology of prepared Cu/Zn-MCM-41-30-30 were studied by scanning electron microscopy (SEM) and results are shown in Fig. 5. The SEM of Cu/Zn-MCM-41 shows uniformed spherical nanoparticles with sizes of <100 nm.

The Lewis and Brönsted acid behaviors of prepared catalyst were verified by FT-IR spectroscopy with the application of pyridine as a molecular probe. A clear distinction between Lewis and Brönsted acid sites of the catalyst was made with this method.

The FT-IR spectra of pyridine adsorbed on Cu/Zn-MCM-41-30-30 before heat treatment (Fig. 6b) shows the contribution of pyridine adducts in the region of 1400–1650 cm^{-1}. In this spectra, the peaks at ~1450 and
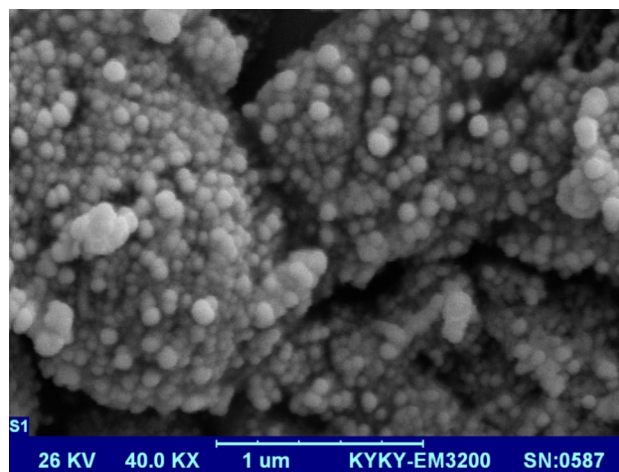
**Fig. 3** The TEM image of the MCM-41 (*a*), Zn-MCM-41-30 (*b*) and Cu/Zn-MCM-41-30-30 (*c*)
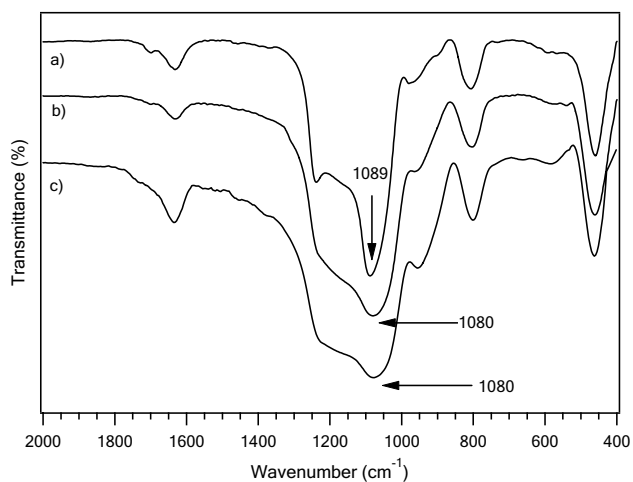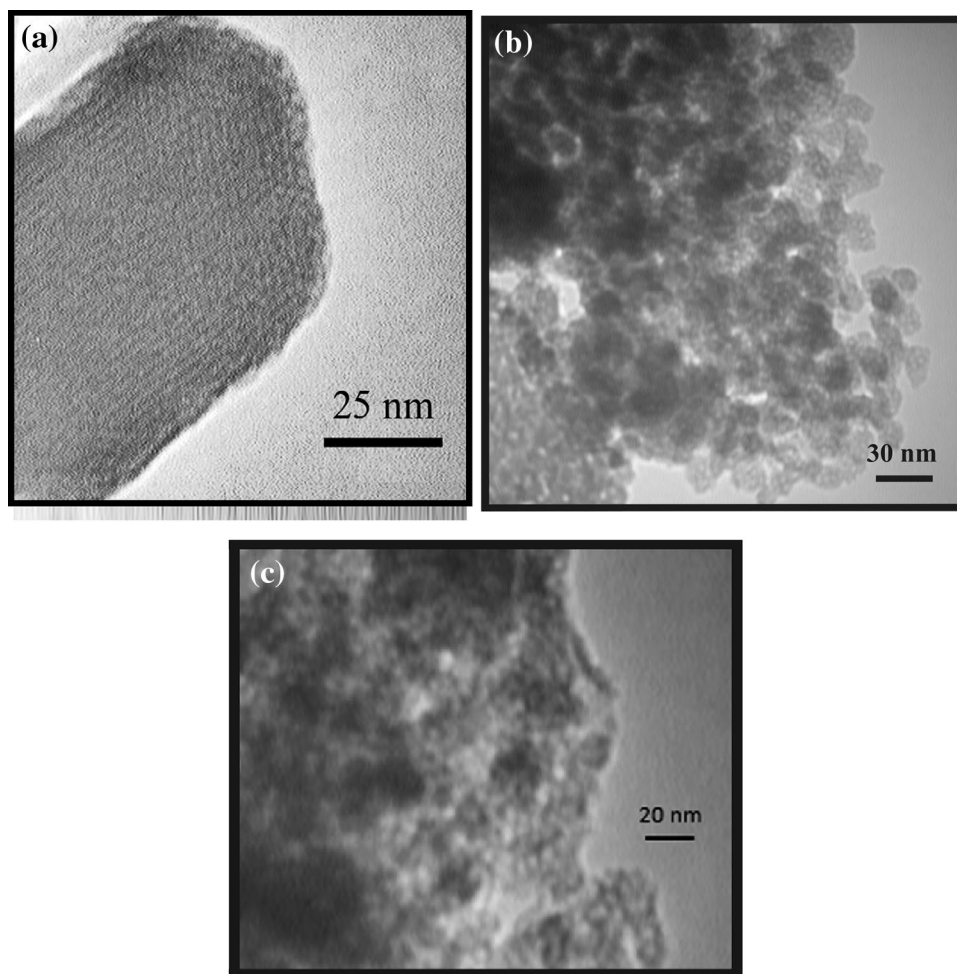
Fig. 4 FT-IR spectra of *(a)* MCM-41, *(b)* Cu-MCM-41-30 and *(c)* Cu–Zn-MCM-41-30-30

Fig. 5 The SEM image of Cu/Zn-MCM-41-30-30

1600 cm^{-1} are attributed to the pyridine bonded Lewis acid sites of the Cu/Zn-MCM-41-30-30. In this analysis, a peak at ~1545 cm^{-1} is assigned to Brönsted acid sites

(corresponds to protonation of pyridine on Brönsted acid sites) that is not found in all spectra. As shown in Fig. 6c–f, with increasing in temperature, Lewis acidity characteristic peaks are still remained at 1448 and 1598 cm^{-1}. These
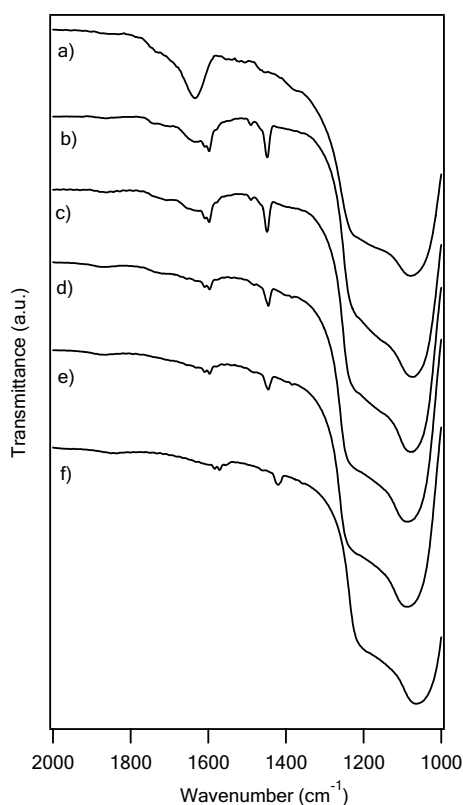
Fig. 6 The FT-IR spectra of *(a)* Cu/Zn-MCM-41-30-30, *(b)* pyridine adsorbed Cu/Zn-MCM-41-30-30 at ambient temperature and pyridine adsorbed Cu/Zn-MCM-41-30-30 heated at *(c)* 100 °C, *(d)* 200 °C, *(e)* 300 °C, *(f)* 400 °C
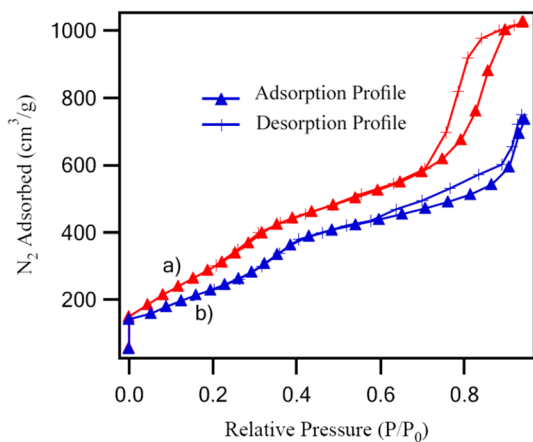
Fig. 7 The nitrogen adsorption–desorption isotherms of MCM-41 (*a*) and Cu/Zn-MCM-41-30-30 (*b*)

results show that Lewis acidity of the catalyst is stronger than its Brönsted acidity [54].

The nitrogen adsorption–desorption isotherms of MCM-41 and Cu/Zn-MCM-41-30-30 are presented in Fig. 7, and the textural properties summarized in Table 1. The results

reported in Table 1 show that the BET surface area and pore volume of the MCM-41 substantially decrease with entrance of the Cu and Zn ions in MCM-41 framework from 1177 to 724.1 m^2/g.

The elemental analysis of the mixed oxide was carried out by an ICP-OES instrument. ICP-OES analysis showed that the amounts of copper, zinc and silicon present in the catalyst were in good agreement with the initial gel composition. By this method, effective Si/Cu and Si/Zn molar ratios in the catalyst sample of Cu/Zn-MCM-41-30-30 was obtained to be equal to 33 and 29, respectively.

In the case of metal modified silica supported catalyzed reactions, the oxidation states of active metals is an important parameter to be considered. As shown in Fig. 8, for X-ray photo electron spectroscopy (XPS) of Cu/Zn-MCM-41-30-30, a Cu $2p_{3/2}$ binding energy of 933.18 eV

Table 1 Textural properties of the catalyst from nitrogen adsorption–desorption isotherms

Samples	BET surface area (m^2/g)	BJH average pore diameter (nm)	Vp (cm^3/g)
MCM-41	1176.96	2.374	1.146
Cu/Zn-MCM-41-30-30	724.10	2.498	0.705
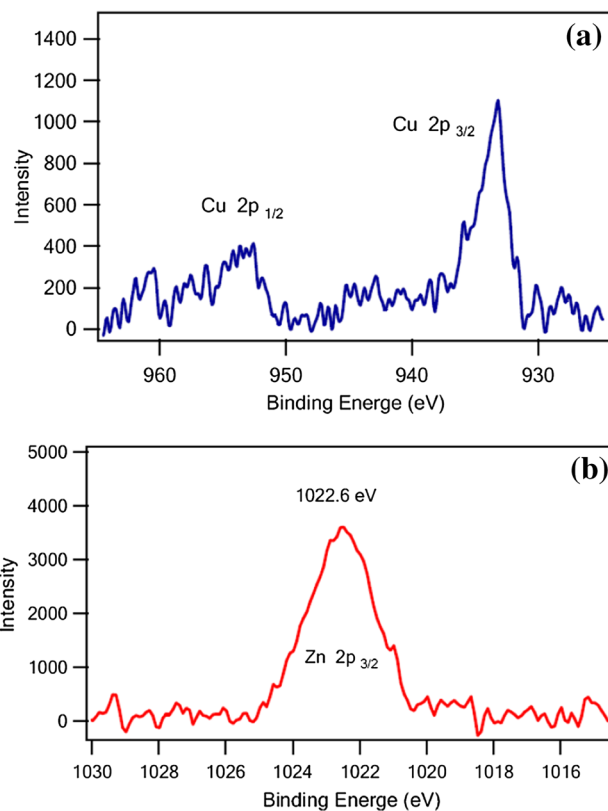
Fig. 8 The Cu (*a*) and Zn (*b*) X-ray photo electron spectroscopy (XPS) of Cu/Zn-MCM-41-30-30

Table 2 The condensation reaction of benzonitrile (1 mmol), aniline (1.1 mmol) and benzoin (1 mmol) under different reaction conditions

Entry	Catalyst (quantity)	Reaction conditions	Time	Yield (%)[a]
1	MCM-41 (20 mg)	Solvent-free, 140 °C	24 (h)	Trace
2	Cu-MCM-41-30 (20 mg)	Solvent-free, 140 °C	24 (h)	81
3	Zn-MCM-41-30 (20 mg)	Solvent-free, 140 °C	24 (h)	80
4	Cu/Zn-MCM-41-30-30 (20 mg)	Solvent-free, 140 °C	16 (h)	85
5	Cu/Zn-MCM-41-60-30 (20 mg)	Solvent-free, 140 °C	24 (h)	84
6	Cu/Zn-MCM-41-30-60 (20 mg)	Solvent-free, 140 °C	24 (h)	85
7	Cu/Zn-MCM-41-30-30 (20 mg)	DMF, 140 °C	24 (h)	80
8	Cu/Zn-MCM-41-30-30 (20 mg)	CH_3CN, reflux	24 (h)	32
9	Cu/Zn-MCM-41-30-30 (20 mg)	CH_2Cl_2, reflux	24 (h)	No reaction
10	Cu/Zn-MCM-41-30-30 (20 mg)	EtOH, reflux	24 (h)	55
11	Cu/Zn-MCM-41-30-30 (20 mg)	MeOH, reflux	24 (h)	35
12	Cu/Zn-MCM-41-30-30 (20 mg)	THF, reflux	24 (h)	No reaction
13	Cu/Zn-MCM-41-30-30 (5 mg)	Solvent-free, 140 °C	24 (h)	40
14	Cu/Zn-MCM-41-30-30 (10 mg)	Solvent-free, 140 °C	24 (h)	55
15	Cu/Zn-MCM-41-30-30 (15 mg)	Solvent-free, 140 °C	18 (h)	73
16	Cu/Zn-MCM-41-30-30 (30 mg)	Solvent-free, 140 °C	16 (h)	85
17	–	Solvent-free, 140 °C	24 (h)	No reaction
18	Cu/Zn-MCM-41-30-30 (20 mg)	Solvent-free, MW (100 W), 90 °C	30 (min)	40
19	Cu/Zn-MCM-41-30-30 (20 mg)	Solvent-free, MW (200 W), 90 °C	20 (min)	75
20	Cu/Zn-MCM-41-30-30 (20 mg)	Solvent-free, MW (300 W), 90 °C	10 (min)	95
21	Cu/Zn-MCM-41-30-30 (20 mg)	Solvent-free, MW (400 W), 90 °C	10 (min)	95
22	Cu/Zn-MCM-41-30-30 (20 mg)	Solvent-free, MW (300 W), 70 °C	30 (min)	70
23	Cu/Zn-MCM-41-30-30 (20 mg)	Solvent-free, MW (300 W), 100 °C	10 (min)	94

[a]Isolated pure products

and the presence of shake up satellite peaks from X-ray photoelectron spectra (XPS) studies confirmed the oxidation state of Cu as 2+, which is in agreement with the XRD data. The peak at about 1021.6 eV is ascribed to the Zn $2p_{3/2}$ of Zn^{2+} ions in Cu/Zn-MCM-41-30-30, which is consistent with values that reported for ZnO [55].

After successful preparation and characterization of Cu/Zn-MCM-41, its catalytic behavior was investigated in the synthesis of tetrasubstituted imidazoles *via* the one-pot three-component reaction of nitriles (**1**), amines (**2**) and benzoins (**3**) (Scheme 1). For this, the reaction of benzonitrile (1 mmol), aniline (1 mmol) and benzoin (1 mmol) was selected as a model reaction and the reaction parameters were optimized under various conditions (Table 2).
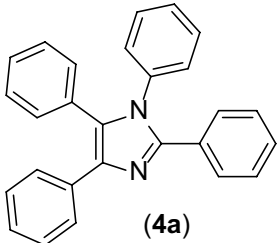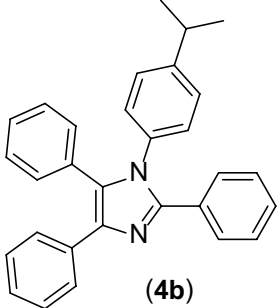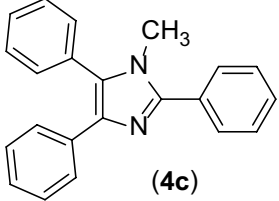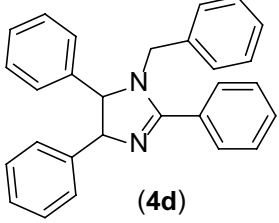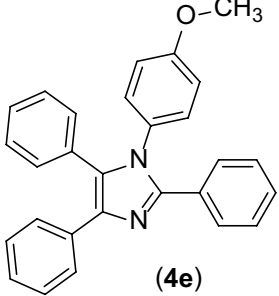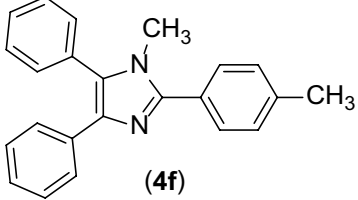
After extensive screening, the best yield and shortest reaction time were obtained with 20 mg of Cu/Zn-MCM-41-30-30 under solvent-free condition at 140 °C, which furnished the corresponding tetrasubstituted imidazole (**4a**) in 85% yield within 16 h (Table 2, entry 4). Increasing the amount of Cu/Zn-MCM-41-30-30 to 30 mg showed no substantial improvement in the yield (Table 2, entry 16), whereas the yield decreased and reaction time increased by the decreasing the amount of the catalyst (Table 2, entries 13, 14 and 15). The reaction did not proceed in the absence of catalyst even after a long time

(24 h) (Table 2, entry 17). Moreover, only a trace amount of products was obtained in the presence of MCM-41 (Table 2, entry 1). Besides, the lower yields of products in longer reaction times were obtained with the application of Cu-MCM-41-30, Zn-MCM-41-30 (Table 2, entries 2 and 3). In the case of Cu/Zn-MCM-41-60-30 and Cu/Zn-MCM-41-30-60 the same yields of products were obtained in longer reaction times (Table 2, entries 5 and 6). These observations establishes the crucial role of Cu/Zn-MCM-41-30-30 in the expedition of the reaction time and the product yield and indicates that the presence of Cu^{2+} and Zn^{2+} ions at the same time in the framework of MCM-41 is necessary to gain the best results.
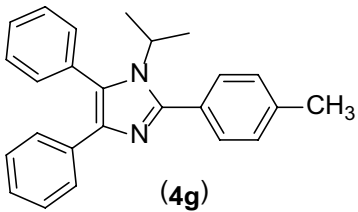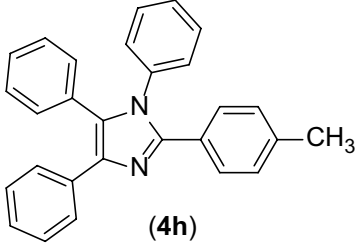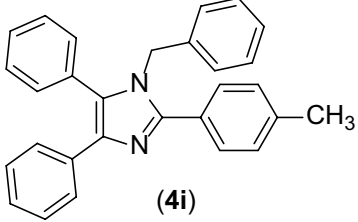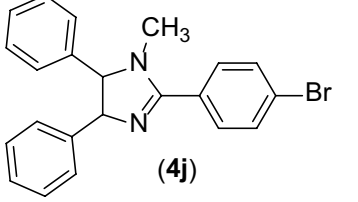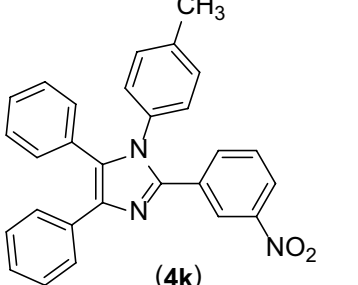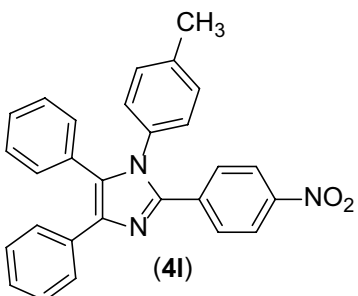
With consideration of the critical role of microwave irradiation on the rate acceleration and yield enhancement of various chemical reactions [56, 57], our methodology was studied under microwave irradiation to improve the overall yield of the reaction and obtained results are summarized in Table 2. As it is shown in Table 2, the best results were obtained at 90 °C with 10 min microwave irradiation with the maximum power of 300 W (Table 2, entry 20). Increasing the temperature and microwave irradiation power did not affect the yield and the reaction time (Table 2, entries 21 and 23).
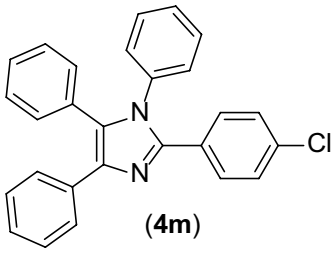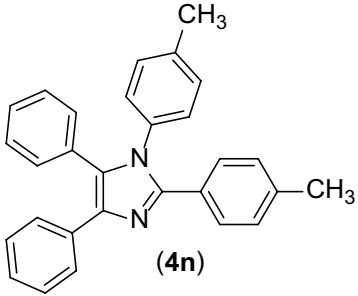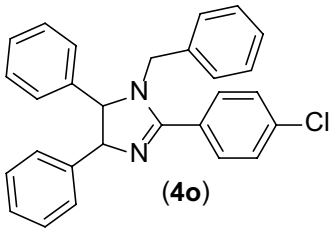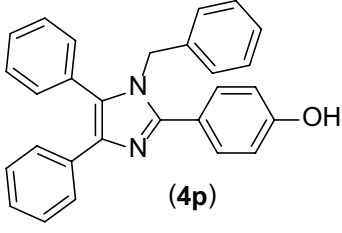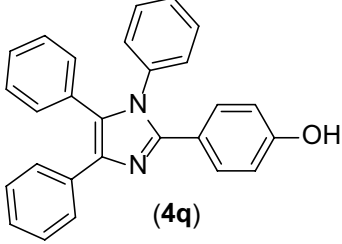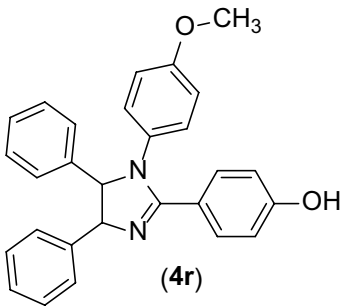
Table 3 The one-pot condensation of nitriles (1 mmol), primary amines (1 mmol) and benzoins (1 mmol) in the presence of Cu/Zn-MCM-41-30-30 (20 mg) under microwave irradiation (300 W) at 90 °C

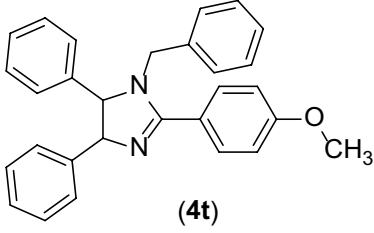| Entry	Product	Time (min)	Yield (%)[a]	M.P. (°C) Found	Reported [references]
1	(4a)	10	95	218–220	219–221 [14]
2	(4b)	10	89	153–155	152–155 [47]
3	(4c)	10	92	146–147	144–146 [14]
4	(4d)	8	95	155–158	157–159 [14]
5	(4e)	8	95	240–242	239–241 [47]
6	(4f)	10	90	214–215	210–213 [14]
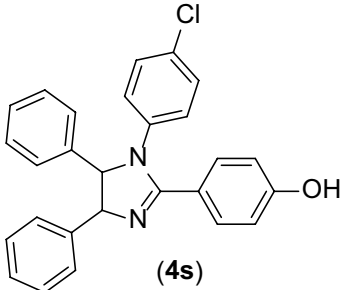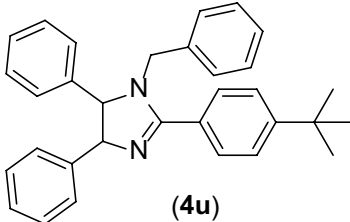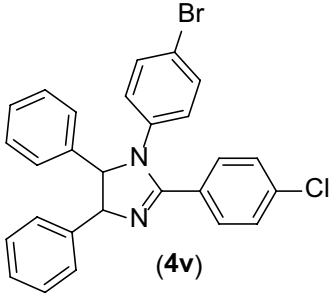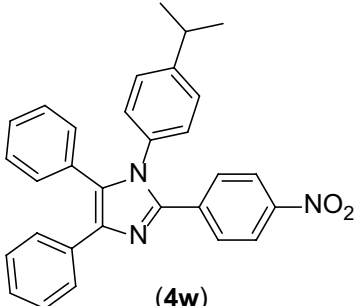
Table 3 (continued)

Entry	Product	Time (min)	Yield (%)[a]	M.P. (°C)	
				Found	Reported [references]
7	(4g)	10	88	150–152	155–156 [14]
8	(4h)	12	90	192–193	191–193 [14]
9	(4i)	10	92	164–166	166–168 [14]
10	(4j)	10	92	200–203	200–203 [14]
11	(4k)	7	90	143–145	145–147 [14]
12	(4l)	7	90	217–220	215–217 [14]
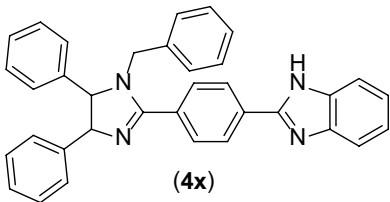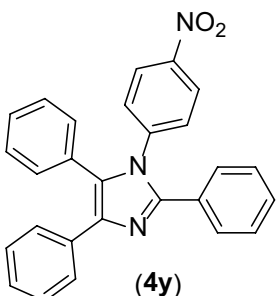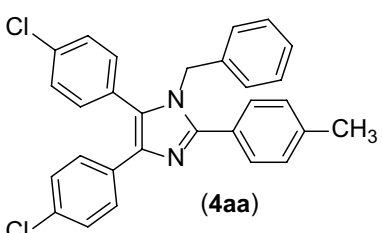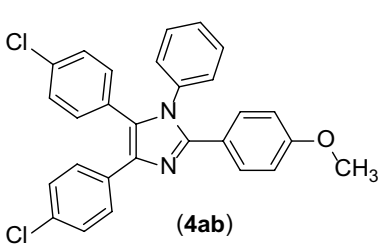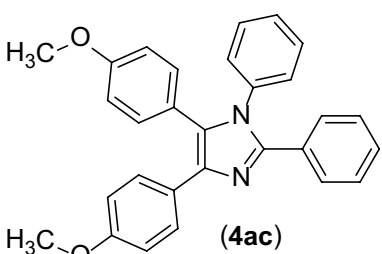
Table 3 (continued)

Entry	Product	Time (min)	Yield (%)[a]	M.P. (°C)	
				Found	Reported [references]
13	(4m)	10	90	160–163	161–163 [14]
14	(4n)	12	92	192–193	194–196 [14]
15	(4o)	9	92	147–149	149–151 [14]
16	(4p)	15	83	134–136	136–138 [14]
17	(4q)	18	88	282–283	283–284 [14]
18	(4r)	12	90	>300	>300 [47]

Table 3 (continued)

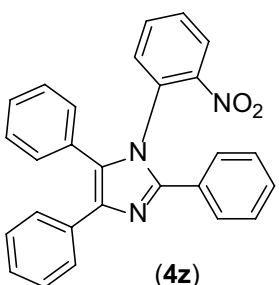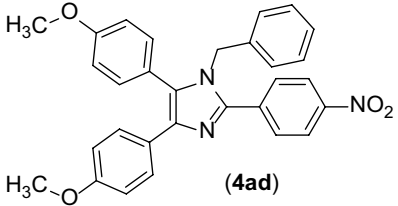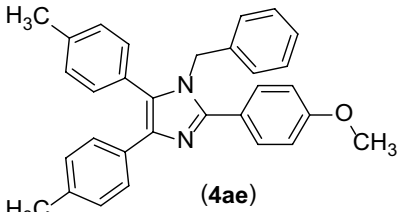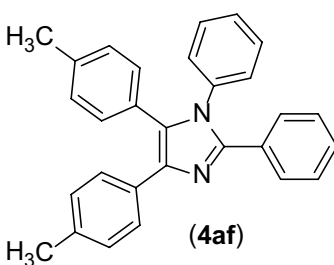| Entry	Product	Time (min)	Yield (%)[a]	M.P. (°C)	
				Found	Reported [references]
19	(4s)	18	82	289–291	290–292 [47]
20	(4t)	13	90	168–170	167–169 [47]
21	(4u)	12	92	175–177	177–179 [47]
22	(4v)	12	90	219–221	217–219 [47]
23	(4w)	7	90	192–194	195–198 [47]

Table 3 (continued)

Entry	Product	Time (min)	Yield (%)[a]	M.P. (°C)	
				Found	Reported [references]
24	(**4x**)	12	92	252–255	254–256 [47]
25	(**4y**)	30	–	–	–
26	(**4z**)	30	–	–	–
27	(**4aa**)	12	91	186–188	185–186 [47]
28	(**4ab**)	18	90	166–167	169–171 [47]
29	(**4ac**)	30	–	–	–

Table 3 (continued)

Entry	Product	Time (min)	Yield (%)[a]	M.P. (°C)	
				Found	Reported [references]
30	(4ad)	30	–	–	–
31	(4ae)	12	90	180–182	183–184 [47]
32	(4af)	14	90	176–178	173–174 [47]

[a]Isolated yield

In the next step, the scope and efficiency of the process were explored under optimized conditions with the one-pot condensation of a broad range of structurally diverse aromatic nitriles (**1**), amines (**2**) and benzoins (**3**) under microwave irradiation (Scheme 1), and the results are displayed in Table 3.

As it can be concluded from Table 3, obtained results are approximately similar to results of the application of TFA [47]. All reactions were completed in short times (7–18 min) and corresponding products were obtained in good to excellent yields (82–95%). Besides, aryl nitriles bearing an electron withdrawing substitution on aromatic ring were reacted faster (Table 2, entries 11, 12 and 23) than the others bearing an electron donating group (Table 2, entries 16, 17, 18, 19 and 20). In addition, the reaction was not proceeded in the case of aromatic primary amines with a strong electron withdrawing groups even after a long time of microwave irradiation (30 min) (Table 2, entries 25 and 26). Application of substituted benzoins was lead to the similar results and halide or alkyl substituted benzoins (Table 2, entries 27, 28, 31 and 32) were successfully converted to desired tetrasunstituted imidazoles whereas only a mixture of unknown products was obtained with

the application of methoxy (as an electron donating group) substituted benzoin even after a long time of microwave irradiation (30 min) (Table 2, entries 29 and 30). These results obviously establishes the similar catalytic efficiency of nano-sized Cu/Zn-modified MCM-41 and TFA, while the application of Cu/Zn-MCM-41 is in combination with some other advantages such as recoverability and reusability of catalyst that will prevent the generation of toxic wastes.

The selectivity of presented method in the condensation of nitriles, amines and benzoins can be explained by a sequence of reactions in which the Cu/Zn-MCM-41 serves two catalytic functions: first, activation of electrophiles with an interaction between Lewis acid sites (Cu^{2+} and Zn^{2+}) and negatively charged parts of electrophiles and the second to enhance the nucleophilicity of nucleophiles with the interaction between positively charged parts of nucleophiles and negatively charged oxygens of Cu/Zn-MCM-41(Scheme 2). This is noteworthy that the presence of electron-positive Cu^{2+} and Zn^{2+} species in the MCM-41 framework leads to the development of higher negative charges on the oxygens.
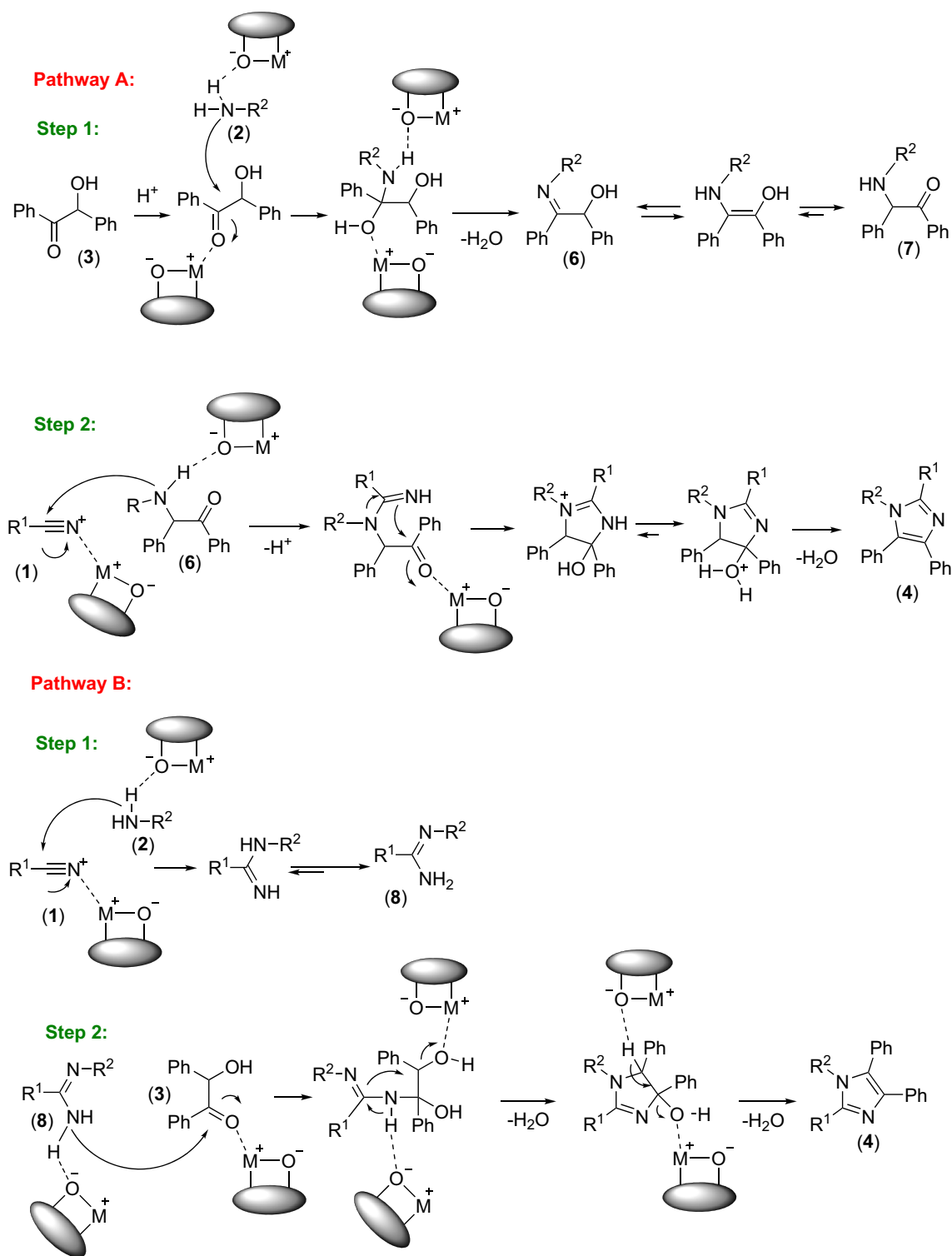
Scheme 2 The suggested mechanism for the one-pot condensation of nitriles (**1**), amines (**2**) and benzoin (**3**) in the presence of nano-sized Cu/Zn-MCM-41-30-30

As it has been previously suggested there are two plausible mechanistic pathways for one-pot condensation of nitriles (**1**), amines (**2**) and benzoins (**3**) [47]. During the first step of pathway A, an imine intermediate (**5**) produces from the condensation of primary amine (**2**) and benzoins (**3**) followed by fast tautomerization of imine (**5**) to an

Fig. 9 The reusability of nano-sized Cu/Zn-MCM-4-30-30 in one-pot condensation of banzonitrile, aniline and benzoin under optimized reaction conditions without calcination (*black* and *red lines*) and with calcination after each time of reuse (*green* and *blue lines*). (Color figure online)
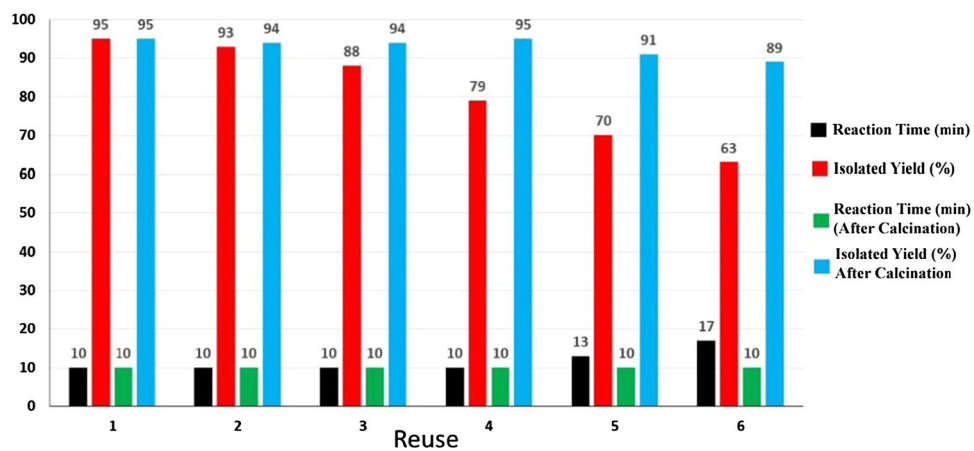
Fig. 10 The XRD [high angle (*a*) and low angle (*b*)] and TEM image of recovered Cu/Zn-MCM-41-30-30 after the 3rd reuse
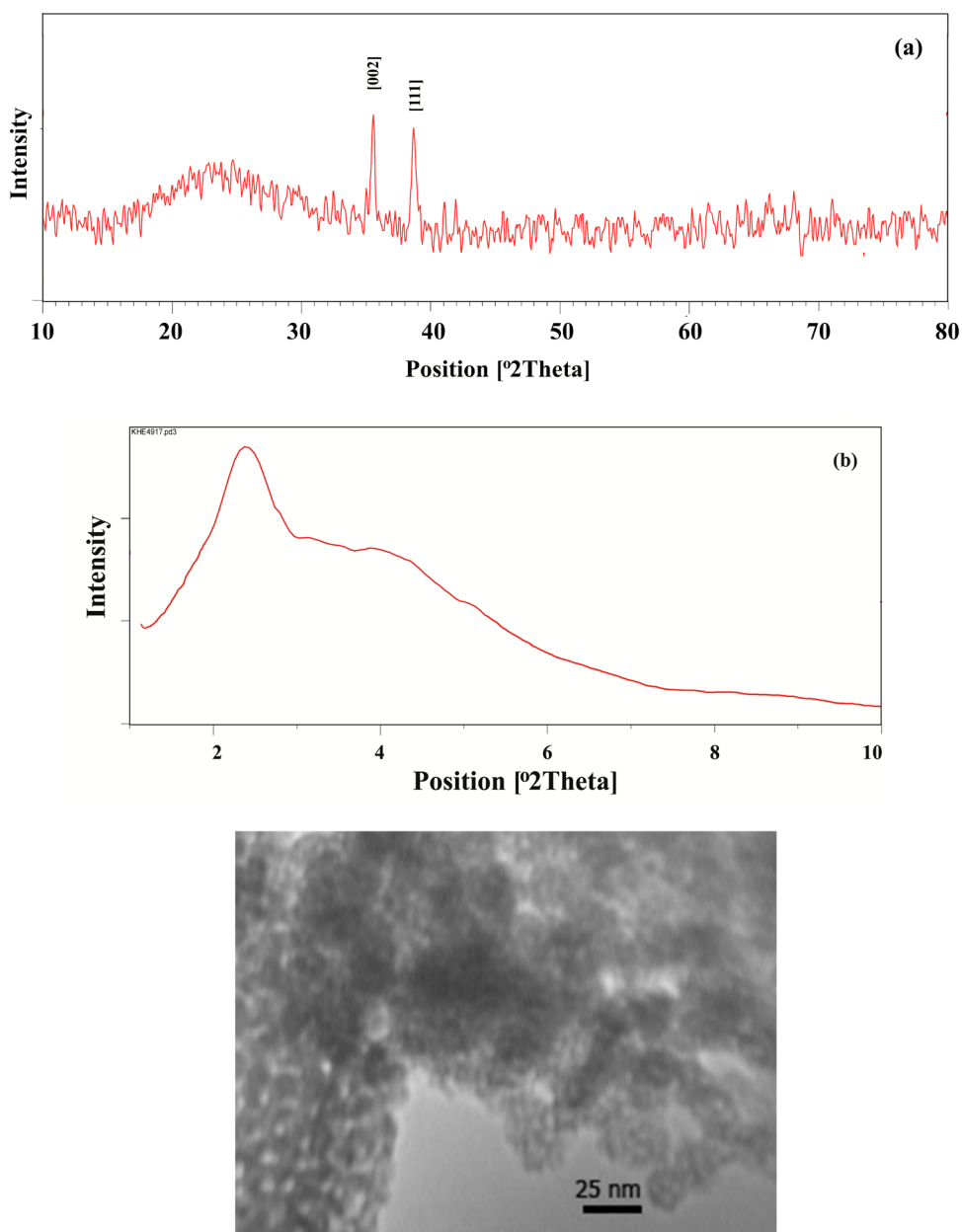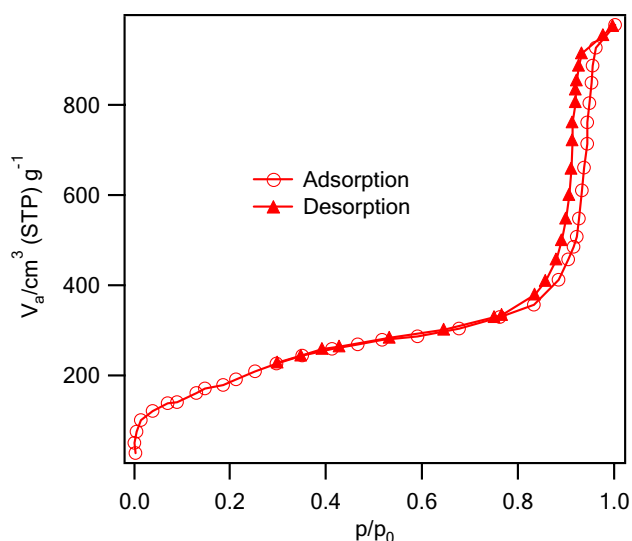
Fig. 11 The nitrogen adsorption–desorption isotherms of recovered Cu/Zn-MCM-41-30-30 after the 3rd reuse and calcination

α-amino carbonyl compound (**6**). In the next step, desired tetrasubstituted imidazole (**4**) will be formed with the nucleophilic attack of α-amino carbonyl compound (**6**) to the nitrile (**1**) that will be followed with an intramolecular nucleophilic cyclization. In the first step of pathway B, an arylamidine (**8**) produces from the nucleophilic attack of amine (**2**) to the nitrile (**1**) followed with the condensation of aryamidine (**8**) with benzoins (**3**) (Scheme **2**).

The recycling and reusability of Cu/Zn-MCM-41-30-30 was examined using the model reaction under the optimized conditions. After completion of the reaction, the reaction mixture was cooled down to room temperature, ethyl acetate was added and obtained mixture was stirred magnetically at 80 °C. The insoluble catalyst was separated with centrifugation, washed with ethyl acetate and dried at 120 °C for 2 h. The catalyst almost completely (>99%) has been recovered from the reaction media. The recovered Cu/Zn-MCM-41 was reused six times and a slight loss of catalytic activity was observed from the third reuse (Fig. 9). It maybe occurs due to the coke depositions and slight amount of copper and zinc leaching from the catalyst. In order to check the effect of coke deposition, the recovered catalyst after the 3rd reuse was calcined at 550 °C for 4 h and obtained catalyst was reused in model reaction and desired product was obtained in 94% yield after 10 min of microwave irradiation. Surprisingly, these results are

too similar to the results of freshly synthesized catalyst. In another study, the Zn and Cu content of recovered catalyst after the 3rd reuse was analyzed by an ICP-OES instrument and obtained results showed that Si/Cu and Si/Zn molar ratios was equal to 32 and 30, respectively. Based on these results it has been concluded that the main reason of loss of catalyst activity after the 3rd reuse is the coke deposition and there is not any evidence about the leaching of Cu^{2+} or Zn^{2+} from the catalyst.

In order to examine the physical stability of recovered catalyst, the meso-structure of recovered Cu/Zn-MCM-41-30-30 after the 3rd reuse was studied by transmittance electron microscope (TEM) and XRD. In TEM image of the recovered catalyst, porosity is well observed in the range of the mesoporous materials (Fig. 10) and there are no differences between the XRD pattern (low angle as well as high angle) of freshly synthesized catalyst and recovered catalyst after the 3rd reuse.

Finally, the textural properties of the recovered catalyst after the 3rd reuse and calcination was studied with BET and XPS methods. The nitrogen adsorption–desorption isotherms of recovered Cu/Zn-MCM-41-30-30 after the 3rd reuse and calcination is presented in Fig. 11, and the textural properties summarized in Table 4. The results reported in Table 4 show that the BET surface area and pore volume of the recovered Cu/Zn-MCM-4-30-30 after the 3rd reuse and calcination is so close to the freshly synthesized Cu/Zn-MCM-4-30-30.
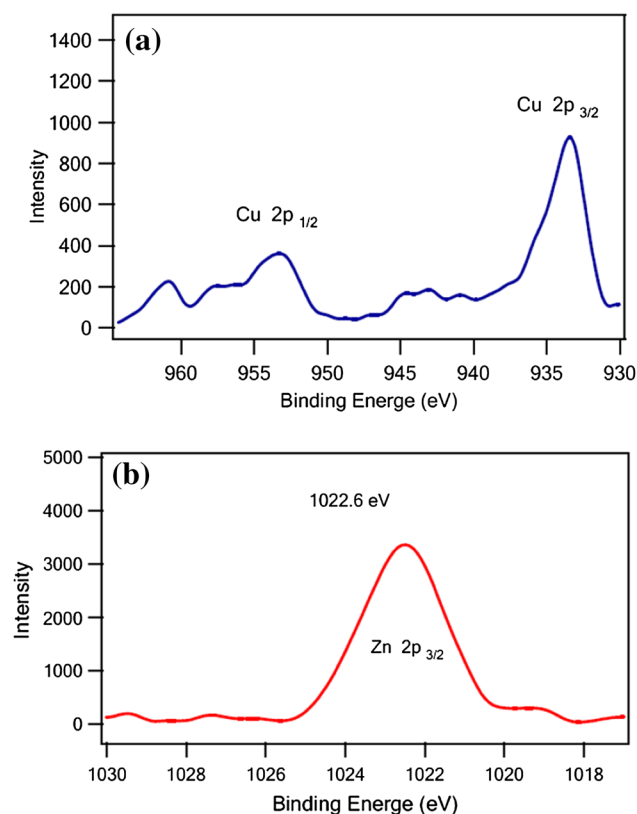
As it is shown in Fig. 12, the X-ray photo electron spectroscopy (XPS) of recovered Cu/Zn-MCM-41-30-30 after the 3rd reuse and calcination is highly similar to the freshly synthesized catalyst and the oxidation states of Zn and Cu are still the same with the freshly synthesized catalyst.

4 Conclusion

In summary, the nano-sized copper/zinc-modified MCM-41 was prepared as a new heterogeneous mesoporous nano-catalyst. The real structure of synthesized catalyst was investigated with IR, SEM, TEM, XRD, ICP-OES and BET methods. The synthesized catalyst was then successfully applied in our recently reported more atom efficient one-pot synthesis of tetrasubstituted imidazoles with the aim of the enhancement in the ecofriendly aspects and avoid of the production of toxic waste. In this method, nitriles were successfully condensed with amines and benzoins in a one-pot approach in

Table 4 Textural properties of the recovered catalyst after the 3rd reuse and calcination from nitrogen adsorption–desorption isotherms

Samples	BET surface area (m^2/g)	BJH average pore diameter (nm)	Vp (cm^3/g)
Recovered Cu/Zn-MCM-41-30-30 after calcination	700.10	2.426	0.691

the presence of Cu/Zn-MCM-41 under microwave irradiation at 90 °C. With the application of Cu/Zn-MCM-41, similar results (reaction times and yields of desired products) were obtained in the comparison with the previously reported catalyst, TFA (a strong and very toxic acid catalyst that is not recoverable). These results stablishes the efficiency of Cu/Zn-MCM-41 to catalyze the one-pot condensation of nitriles, amines and benzoins similar to a strong acid catalyst (TFA). Some promising points for the presented methodology are its versatility, physical and chemical stability of synthesized catalyst, high yields of products, Recoverability and reusability of applied catalyst, short reaction times, avoid of the toxic waste production, ease of product isolation, application of highly efficient energy source, and finally good agreement with some aspects of green chemistry.

References

1. P.T. Anastas, J.C. Warner, *Green Chemistry: Theory and Practice*. (Oxford University Press, Oxford, 1998)
2. C.Y. Lai, Y.S. Thermodyn, J. Catal. **5**, e124 (2013)
3. T. Cheng, D. Zhang, H. Li, G. Liu, Green Chem. **16**, 3401 (2014)
4. M. Heitbaum, F. Glorius, I. Escher, Angew. Chem. Int. Ed. **45**, 4732 (2006)
5. H. Ngo, W. Lin, Top. Catal. **34**, 85 (2005)
6. J.M. Thomas, R. Raja, Acc. Chem. Res. **41**, 708 (2008)
7. M. Abdollahi-Alibeik, A. Rezaeipoor-Anari, Catal. Sci. Technol. **4**, 1151 (2014)
8. M. Abdollahi-Alibeik, M. Pouriayevali, Catal. Commun. **22**, 13 (2012)
9. B. Chakraborty, B. Viswanathan, Catal. Today **49**, 253 (1999)
10. J. Demel, J. Cejka, P. Stepnicka, J. Mol. Catal. A **274**, 127 (2007)
11. J.C. Juan, J. Zhang, M.A. Yarmo, J. Mol. Catal. A **267**, 265 (2007)
12. M.H. Al-Hazmi, A.W. Apblett, Catal. Sci. Technol. **1**, 621 (2011)
13. C.W. Jiang, X. Zhong, Z.H. Luo, RSC Adv. **4**, 15216 (2014)
14. X. Dong, Y. Hui, S. Xie, P. Zhang, G. Zhou, Z. Xie, RSC Adv. **3**, 3222 (2013)
15. F. Farzaneh, E. Zamanifar, C.D. Williams, J. Mol. Catal. A **218**, 203 (2004)
16. J.S. Choi, S.S. Yoon, S.H. Jang, W.S. Ahn, Catal. Today **111**, 280 (2006)
17. L. Wang, A. Kong, B. Chen, H. Ding, Y. Shan, M. He, J. Mol. Catal. A **230**, 143 (2005)
18. S. Vetrivel, A. Pandurangan, J. Mol. Catal. A **227**, 269 (2005)
19. V.C. Corberan, M.J. Jia, J. El-Haskouri, R.X. Valenzuela, D. Beltran-Porter, P. Amoros, Catal. Today **91**, 127 (2004)
20. A. Szegedi, M. Popova, V. Mavrodinova, M. Urban, I. Kiricsi, C. Minchev, Microporous Mesoporous Mater. **99**, 149 (2007)
21. S. Higashimoto, Y. Hu, R. Tsumura, K. Iino, M. Matsuoka, H. Yamashita, Y.G. Shul, M. Che, M. Anpo, J. Catal. **235**, 272 (2005)
22. M.R. Grimmett, in *Comprehensive Heterocyclic Chemistry II*, ed. by A.R. Katritsky, E.F.V. Scriven (Pergamon, Oxford, 1996), pp. 77–220
23. M. Misono, Chem. Commun. **13**, 1141 (2001)
24. J.W. Black, G.J. Durant, J.C. Emmett, C.R. Ganellin, Nature **248**, 65 (1974)
25. U. Ucucu, N.G. Karaburun, I. Iskdag, Farmaco **56**, 285 (2001)
26. S. Samai, G.C. Nandi, P. Singh, M.S. Singh, Tetrahedron **65**, 10155 (2009)
27. S.R. Sarkar, C. Mukhopadhyay, Eur. J. Org. Chem. **6**, 1246 (2015)
28. D.V. Paone, A.W. Shaw, Tetrahedron Lett. **49**, 6155 (2008)
29. A. Shaabani, E. Rahmati, E. Farhangi, Z. Badri, Catal. Commun. **8**, 1149 (2007)
30. B.F. Mirjalili, A.H. Bamoniri, L. Zamania, Sci. Iran. **19**, 565 (2012)
31. H. Veisi, A. Khazaei, L. Heshmati, S. Hemmati, Bull. Korean Chem. Soc. **33**, 1231 (2012)
32. A.R. Khosropour, Ultrason. Sonochem. **15**, 659 (2008)
33. H. Sharghi, M. Aberi, M.M. Doroodmand, Mol. Divers. **19**, 77 (2015)
34. M. Xia, Y.D. Lu, J. Mol. Catal. A **265**, 205 (2007)
35. A. Akbari, Tetrahedron Lett. **57**, 431 (2016)
36. S.J. Saghanezhad, A.R. Kiasat, Org. Chem. Res. **2**, 57 (2016)
37. A. Olyaeia, Z. Derikvand, F. Noruzian, M. Sadeghpour, Iran. Chem. Commun. **4**, 337 (2016)
38. D. Wang, Z. Li, X. Huang, Y. Li, ChemistrySelect **4**, 664 (2016)
39. S.U. Bhat, R.A. Naikoo, M.A. Mir, R. Tomar, Int. J. Curr. Pharm. Res. **8**, 36 (2016)
40. M.A. Zolfigol, S. Baghery, A.R. Moosavi-Zare, S.M. Vahdat, RSC Adv. **5**, 32933 (2015)
41. S. Yadegarian, A. Davoodnia, A. Nakhaei, Orient. J. Chem. **31**, 573 (2015)
42. B.P. Reddy, V. Vijayakumar, M.V. Arasu, N.A. Al-Dhabi, Molecules **20**, 19221 (2015)
43. Kh.. Pourshamsian, J. Solid Mater. **2**, 1 (2014)
44. V. Kannan, K. Sreekumar, J. Mol. Catal. A **376**, 34 (2013)

45. Y. Ran, M. Li, Z.-Z. Zhang, Molecules **20**, 20286 (2015)
46. K. Khan, Z.N. Siddiqui, Ind. Eng. Chem. Res. **54**, 6611 (2015)
47. A. Khalafi-Nezhad, M. Shekouhy, H. Sharghi, J. Aboonajmi, A. Zare, RSC Adv. **6**, 67281 (2016)
48. M. Shekouhy, A. Khalafi-Nezhad, Green Chem. **17**, 4815 (2015)
49. M. Shekouhy, A. Moaddeli, A. Khalafi-Nezhad, Res. Chem. Intermediat. **46**, 3805 (2016)
50. F. Bahrami, F. Panahi, R. Yousefi, M.B. Shahsavani, A. Khalafi-Nezhad, RSC Adv. **6**, 5915 (2016)
51. F. Panahi, N. Zarnaghash, A. Khalafi-Nezhad, New J. Chem. **40**, 1250 (2016)
52. S. Khajeh Dangolani, F. Panahi, M. Nourisefat, A. Khalafi-Nezhad, RSC Adv. **6**, 92316 (2016)
53. M. Shekouhy, A. Maoudi Sarvestani, S. Khajeh, A. Khalafi-Nezhad, RSC Adv. **5**, 63705 (2015)
54. M. Abdollahi-Alibeik, A. Moaddeli, New J. Chem. **39**, 2116 (2015)
55. G. Morettit, G. Fierro, M. Lo Jacono, P. Porta, Surf. Interface Anal. **14**, 325 (1989)
56. A. Zare, A. Parhami, A.R. Moosavi-Zare, A. Hasaninejad, A. Khalafi-Nezhad, M.H. Beyzavi, Can. J. Chem. **87**, 416 (2009)
57. C.O. Kappe, Angew. Chem., Int. Ed. **43**, 6250 (2004)